Weld Seam Tracking and Simulation of 3-Axis Robotic Arm for Performing Welding Operation in CAD Environment

B B V L Deepak[1,*], C A Rao[1] and B M V A Raju[1]
Automation Lab., Dept. of Industrial Design, National Institute of Technology- Rourkela, India
Email: bbv@nitrkl.ac.in

Abstract: In this paper, a 3-axis robotic arm has been modelled using CAD tool for performing welding operations. For the developed robotic arm, forward & inverse kinematic analyses have been performed to move the weld torch in the desired trajectory. A new seam tracking methodology, named sewing technique has been introduced for the welded joints available in Computer Aided Design (CAD) environment. This methodology, gives the seam path by drawing a line through the adjacent centroids of curve fitted in the weld joint volume. Obtained geometric path and kinematic constraints are given as input to the modelled robot for performing welding operation followed by desired trajectory. Validation of the developed methodology has been done through simulation results while performing welding operations for different weld profiles.

Key words: CAD, Robotic arm, forward & inverse kinematics, weld seam tracking, trajectory generation

1. Introduction

Most of the construction machinery parts are welded structures and arc welding technique is mainly used to produce such products. The welding process has been automated from the last few decades through the use of robots and 90% or more of total weld lines are currently automated.

Bae et al. (2002) performed an extensive research work on automated welding robot applications and concluded that exact weld position and orientation of a work piece and its detailed surface geometry are necessary for the robot guidance. Among various sensors used for weld seam tracking, laser sensor technology gives accurate solutions. This technology is probably the most powerful form of sensory feedback and it can provide 3D geometrical information of any arbitrary shaped work pieces in detail without requiring any contact with the work piece. A vision sensor is used in automatic welding to acquire image patterns of a three dimensional manner and two dimensional image patterns were tested using neural network (Yoo & Na 2003). Gao &Na (2005) performed a set of experiments to evolve weld position equations by estimating the centroid of the weld pool pictures. Ye et al. (2013) presented a passive vision-based robotic welding system, which can realize the seam tracking function for pulse-MAG welding.

Kim et al. (2003) obtained a relationship among the input welding process parameters and the output as the weld penetration. Using these relations, robotic welding process (arc welding) can be controlled in order to achieve desired weld quality. Fuzzy linear regression approach was employed by Xue et al. (2005) to determine the relationship between input as process parameters and output as weld quality in the robotic arc welding process. The input parameters are welding current, arc voltage, wire diameter, and torch speed and the weld quality they measured in terms weld bead width. Nagesh & Datta (2013) had come out with a set of empirical relations related to the process parameters and the bead shape. They considered the input parameters as the welding process variables and the output as the weld bead geometry in terms of bead front height & width and back height & width. Several number of experiments have been performed in order to establish a relationship among the robotic arc welding process variables (Dhas & Kumanan, 2011). Later they implemented genetic algorithm and particle swarm optimization techniques to obtain optimal weld parameters. Katherasan et al. (2014) addressed a neural network based regression tool to predict weld bead geometry with respect to process parameters in flux cored arc welding process and then implemented particle swarm optimization to find optimal process parameters. The past research work concerned primarily on weld geometry/seam tracking or relation among very few process related parameters. But these involves more complications while performing welding operations. The proposed system is a simple seam tracker can be used for continuous and long seam welding. It can be controlled and monitored remotely without human operation, thereby reducing the risk of hazards. Since the welding operation can be monitored initially in the CAD environment, the produced weldments would be uniform, superior and the cycle time can be faster in comparison to the presently available systems.

2. Analytical Kinematic Models of 3-Axis Manipulator

In this investigation, a 3-axis manipulator has been considered for performing welding operation in virtual environment. 3-axis are correspond to base rotation, elbow rotation and wrist pitch as shown in Fig.1. While the tool of the robot follows the seam path, the position (X, Y, and Z) of the weld torch will vary without varying the roll angle of the torch. Since the roll angle of the weld electrode will not influence the welding

operation, the roll of the tool has not been considered throughout this analysis. It means the roll angle of the weld torch is fixed to a specific value.

In forward kinematic analysis, for given link lengths and joint angles, end-effector's position and orientation with respect to base are to be calculated. Where as in the inverse kinematic analysis is, for given position and orientation of end-effector, joint parameters are to be obtained. A detailed explanation of forward and inverse kinematic models of a robotic manipulator is provided by Elias et al. (2012) and Parhi et al. (2013)

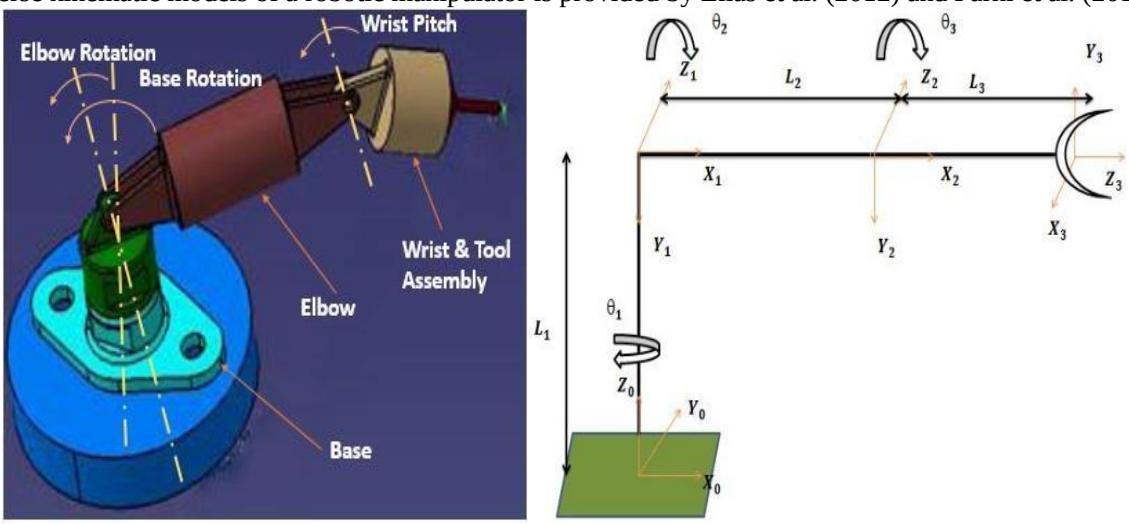

Figure.1: CAD model of robot, its coordinate frames

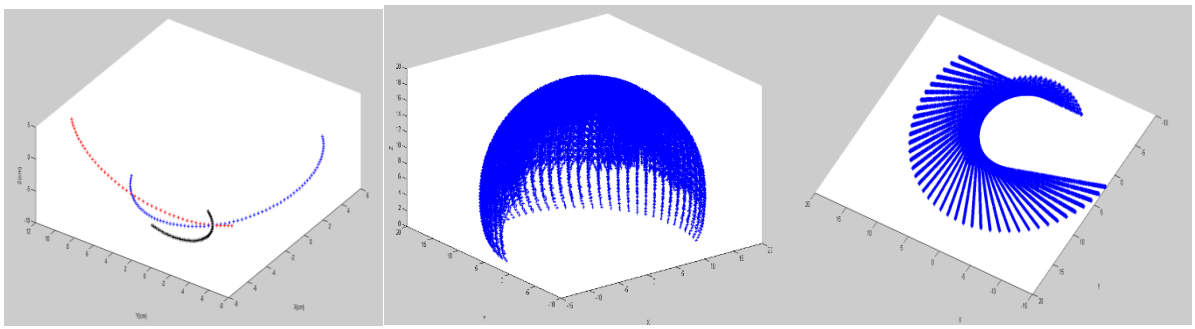

Figure.2: Variation of end-effector position when all joint angles are varied uniformly and other joints are at fixed angle and its work volume [All dimensions are in cm.]

The developed 3-axis robot model, its coordinate frames and its work volume are shown in Figs.1&2 and the specification of the manipulator is illustrated in Table.1.

Table.1 Specification of the developed Robot

Specification	**Value**	**Units**
Number of axes	3	
No of Links	3	
Lengths of Link1, Link 2 and Link 3	70,100,70	mm
Work Envelope	Body Rotation : 360 Elbow Rotation :180 to -180 Wrist Rotation : 90,270	degrees

2.1. Forward Kinematic Model

Forward kinematics generally refers to position analysis of the end-effector. So the forward kinematic analysis is equivalent to a determination of arm matrix by combining transformation matrices as represented in Eq. (1). The set of link coordinates assigned using DH convention is then transformed from coordinate frame (N_i) to (N_{i-1}). Using a homogeneous coordinate transformation matrix, the relation between adjacent links is given in Eq.(1).

$$T_i = Rot(z, \theta_i) * Trans(0,0,d_i) * Trans(a_i,0,0) * Rot(x, \alpha_i)$$

$$= \begin{bmatrix} C\theta_i & -S\theta_i C\alpha_i & S\theta_i S\alpha_i & a_i C\theta_i \\ S\theta_i & C\theta_i C\alpha_i & -C\theta_i S\alpha_i & a_i S\theta_i \\ 0 & S\alpha_i & C\alpha_i & d_i \\ 0 & 0 & 0 & 1 \end{bmatrix} \quad (1)$$

Here C_i=cos(θ_i), S_i=sin(θ_i)

On substituting the kinematic parameters illustrated in Table 1, individual transformation matrices T_0^1 to T_3^4 can be found and the global transformation matrix T_0^4 of the robot arm is found according to the Eq. (2).

$T_{base}^{tool} = T_{base}^{wrist} * T_{wrist}^{tool}$

Where $T_{base}^{wrist} = T_0^1 * T_1^2$

$T_{wrist}^{tool} = T_2^3 * T_3^4$

$$T_{base}^{tool} = \begin{bmatrix} m_x & n_x & o_x & p_x \\ m_y & n_y & o_y & p_y \\ m_z & n_z & o_z & p_z \\ 0 & 0 & 0 & 1 \end{bmatrix} = \begin{bmatrix} R(\theta)_{3x3} & P_{3x1} \\ 0 & 1 \end{bmatrix} \quad (2)$$

Where (p_x, p_y, p_z) represents the position and $R(\theta)_{3x3}$represents the rotation matrix of the end effector. From this transformation matrix, the position (translation) of end-effector with reference to base frame as a function of the joint angles is depicted in Figure3.

Tool configuration is six-dimensional because arbitrary specified by three position co-ordinates (x, y, z) and orientation co-ordinates (yaw, pitch, roll).

$$X = \begin{Bmatrix} p_x \\ p_y \\ p_z \\ y \\ p \\ r \end{Bmatrix} = \begin{Bmatrix} c_1(a_2c_2 + a_3c_{23} - d_4s_{23}) \\ s_1(a_2c_2 + a_3c_{23} - d_4s_{23}) \\ d_1 - a_2s_2 - a_3s_{23} - d_4c_{23} \\ -[exp(\theta_4)/\pi]c_1s_{23} \\ -[exp(\theta_4)/\pi]s_1s_{23} \\ -[exp(\theta_4)/\pi]c_{23} \end{Bmatrix} \quad (3)$$

Since the roll angle θ_4 is fixed, tool orientation will change according to base rotation, elbow rotation and wrist pitch during its operation.

2.2. Inverse Kinematic Analysis

In a robotic arm, joint variables are the independent variables and will change with respect to the different reference frames. In this investigation, a simple analytical/ geometrical approach method implemented to solve the inverse kinematic problem. For the considered 3-axis manipulator, Fig.2 shows the elbow, wrist position for the same end effector position. Since the wrist angle (θ_2) depends on elbow angle(θ_3), there will be two wrist angles correspond to each angle as shown in the Fig.2.

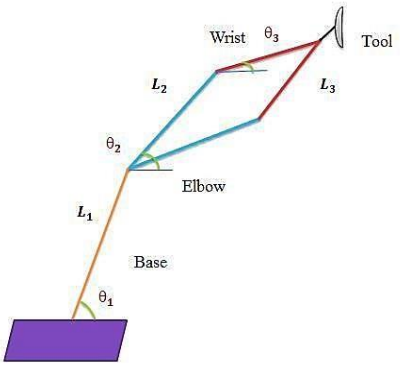

Figure.3: Elbow & Wrist position for given end-effector position

The base angle can be determined by Eq. (4)

Base angle $\theta_1 = arctan\ (P\_Y/P\_X)$ (4)

After finding the base angle, the 3R problem can be converted into 2R planar problem. The two wrist angles ($\pm\theta_3$) can be found for the same tool position as follows:

The manipulator tip point global position is represented by Eqs. (5) & (6)

$Y = l_2 cos\theta_1 + l_3 \cos(\theta_2 + \theta_3)$ (5)

$Z = l_2 sin\theta_1 + l_3 \sin(\theta_2 + \theta_3)$ (6)

Therefore

$Y^2 + Z^2 = l_2^2 + l_3^2 + 2l_2l_3cos\theta_3$

$$cos\theta_3 = \frac{Y^2 + Z^2 - l_2^2 - l_3^2}{2l_2l_3} \Rightarrow \theta_3 = cos^{-1}\left(\frac{Y^2 + Z^2 - l_2^2 - l_3^2}{2l_2l_3}\right) \quad (7)$$

To find θ_2 using atan2 function is represented by Eq. (3.17)

$$\theta_2 = \pm atan2\sqrt{\frac{(l_2 + l_3)^2 - (Y^2 + Z^2)}{(Y^2 + Z^2) - (l_2 - l_3)^2}} \quad (8)$$

The $\pm$ is because of the square root, which gives two solutions. These two solutions are called as elbow up and elbow down.

The joint angle θ_2 for elbow up position is given by Eq. (3.18) and for elbow down position is given by Eq. (9)

$$\theta_2 = atan2\frac{Z}{Y} + atan2\left(\frac{l_3 sin\theta_3}{l_2 + l_3\cos\theta_3}\right) \quad (9)$$

$$\theta_2 = atan2\frac{Z}{Y} - atan2\left(\frac{l_3 sin\theta_3}{l_2 + l_3\cos\theta_3}\right) \quad (10)$$

Fixed Tool roll angle $\theta_4 = \pi * ln\sqrt{(y^2 + p^2 + r^2)}$ (11)

3. Sewing Technique for Obtaining Seam Path

From the existed CAD model, it is very easy to know the geometry where to be welded. In this approach, control points are considered along the length/ periphery of the welding joint. The control points of opposite edges are connected by a curve and along the entire length we have to draw the curves. These curves representation is shown in Fig.3. By joining the centroids of each curve we will get a path that path is nothing but weld seam path. This technique is known as sewing technique and it can be modelled by generative shape design module in CATIA.

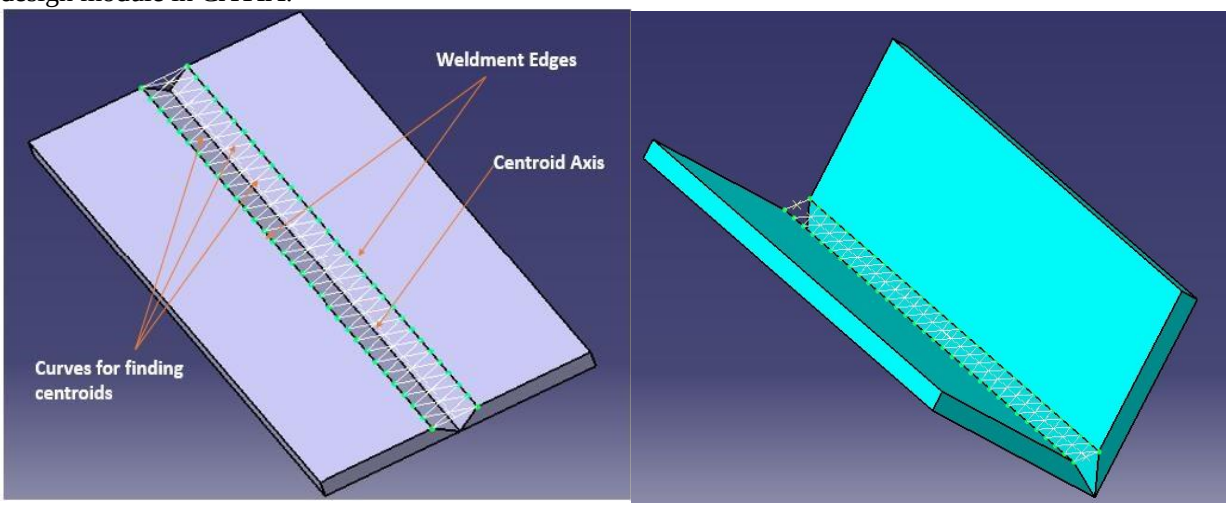

Figure.4: Sewing technique to find seam path for plate and L-Joint

By knowing weld seam coordinates it is very easy to obtain the joint angles of a robot using inverse kinematic model. Finally along the weld seam path and it will perform the welding operation. The key feature of this approach is that, the initial and end positions of the weld seams can be obtained easily. Because of this the robot can be controlled flexibly, during welding operation.

3. Simulation of Welding Operation

The obtained geometric path (seam path) and kinematic constraints will be given as input to the developed robotic arm for performing welding operation. The robot is known about the input parameters such as electrode consumption rate and weld torch speed prior to perform welding operation.

In this analysis the trajectory planning is performed according to the 3rd order cubic spline interpolation.

For the cubic spline trajectory

$(t) = a1 * t^3 + a2 * t^2 + a3 * t + a4$ (11)

The constant values can be obtained while subjected to following boundary conditions:

- At $t=0$, $a4 = \theta_0\ (given)\ and\ v_0 = a3/t$
- At t=1, $a1 + a2 + a3 + \theta_0 = \theta_f$
- $v_f = (3a1 * t^2 + 2a2 * t + a3)/t$
- $a_f = (6a1 * t + 2a2)/t^2$

In experimental analysis, a program has been generated for inverse kinematic solution. This program is written in VB script. Robot welding operation is performed in virtual environment to validate developed methodology.

Case 1: Welding operation of butt joint

Importing Coordinate Data from CAD to Excel and Excel to MAT Lab

Weld seam coordinate data from sewing technique can be extracted to Excel. The program has been developed in VB script to extract the CATIA point coordinate data into Excel. The seam path obtained by the sewing technique for the considered butt joint is illustrated in Table.2.

Table.2: Shows the point coordinate data of weld seam path**.**

Co-ordinate	X	Y	Z	Co-ordinate	X	Y	Z
1	120	90	80	**16**	1.034483	105.5172	61.89655
2	112.069	91.03448	78.7931	**17**	-6.89655	106.5517	60.68966
3	104.1379	92.06897	77.58621	**18**	-14.8276	107.5862	59.48276
4	96.2069	93.10345	76.37931	**19**	-22.7586	108.6207	58.27586
5	88.27586	94.13793	75.17241	**20**	-30.6897	109.6552	57.06897
6	80.34483	95.17241	73.96552	**21**	-38.6207	110.6897	55.86207
7	72.41379	96.2069	72.75862	**22**	-46.5517	111.7241	54.65517
8	64.48276	97.24138	71.55172	**23**	-54.4828	112.7586	53.44828
9	56.55172	98.27586	70.34483	**24**	-62.4138	113.7931	52.24138
10	48.62069	99.31034	69.13793	**25**	-70.3448	114.8276	51.03448
11	40.68966	100.3448	67.93103	**26**	-78.2759	115.8621	49.82759
12	32.75862	101.3793	66.72414	**27**	-86.2069	116.8966	48.62069
13	24.82759	102.4138	65.51724	**28**	-94.1379	117.931	47.41379
14	16.89655	103.4483	64.31034	**29**	-102.069	118.9655	46.2069
15	8.965517	104.4828	63.10345	**30**	-110	120	45

For the point data imported in Excel, inverse kinematic solutions can be obtained using MATLAB program. The 3D plot of the end-effector trajectory for the generated weld seam is shown in Fig.5.

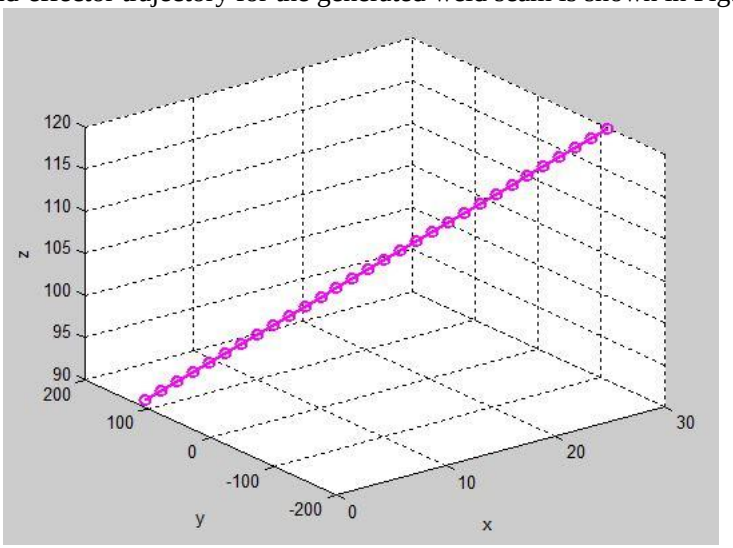

Figure 5: 3D plot for the weld seam coordinate data

Fig.4 shows the robot is performing welding task in virtual environment while following its kinematic constraints as discussed above. The considered weld joints thickness is 5mm. and its length is 15cm.

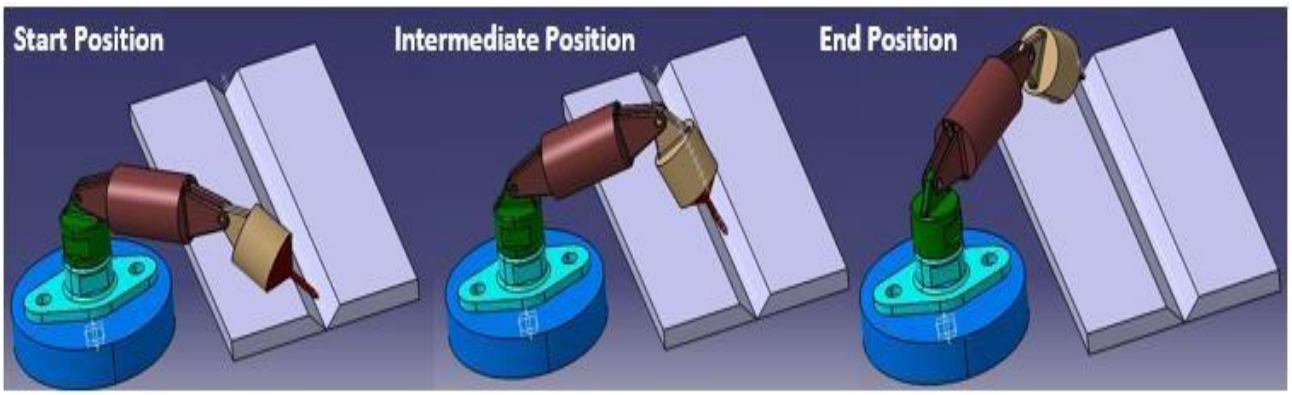

Figure.4: Robot following seam path for performing Welding operation of butt joint

Case 2: Welding operation of L - joint

In the similar manner as discussed above, Fig.5 shows the robot is performing welding task in virtual environment while following its kinematic constraints as discussed above. The considered weld joints thickness is 5mm. and its length is 15cm.

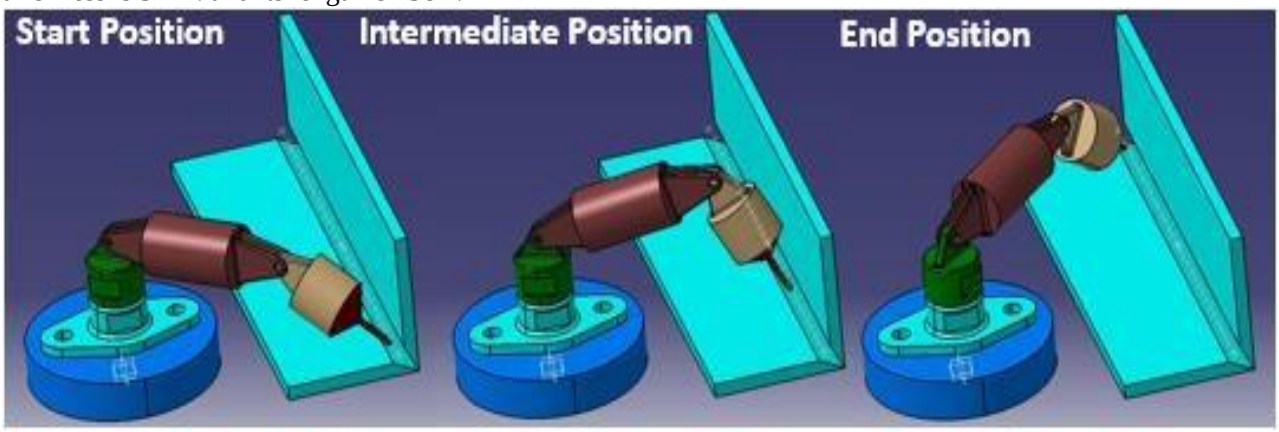

Figure.5: Robot following seam path for performing Welding operation of L - joint

3.1. Comparison with Previous Work

Some of the past research work as illustrated in Table 2 represents the various methodologies for performing seam tracking and welding operation. A detailed comparison has been provided in Table 2.

Table 2: Comparison with previous work

Past work	Method for weld seam Tracking	Seam Initial & Final Position detection	Robot Trajectory planning & Kinematic constraints
Bae et al. (2002)	Optical sensing system	✓	X
Yoo & Na (2003)	Laser sensing system	X	✓
Gao & Na (2005)	Passive vision system	X	X
Kiddee et al. (2014)	X	✓	X
Dahari & Tan (2011)	X	X	✓
Kumar et al. (2013)	CAD based	X	✓
Current study	CAD based	✓	✓

4. Conclusion

This investigation has been carried out to simulate the 3-axis robotic arm in CAD environment for performing welding operation while following the weld seam path and its kinematic constraints. A new seam tracking methodology, named sewing technique has been introduced for the welded joints available in Computer Aided Design (CAD) environment. Validation of the developed methodology has been done through simulation results while performing welding operations for different weld profiles. Still this work is in primary stage (simulation) and requires validation with real-time welding operation.

References

1. Bae, K. Y., Lee, T. H., & Ahn, K. C. (2002). An optical sensing system for seam tracking and weld pool control in gas metal arc welding of steel pipe. Journal of Materials Processing Technology, 120(1), 458-465.
2. Dahari, M., & Tan, J. D. (2011, April). Forward and inverse kinematics model for robotic welding process using KR-16KS KUKA robot. In Modeling, Simulation and Applied Optimization (ICMSAO), 2011 4th International Conference on (pp. 1-6). IEEE.
3. Dhas, J. E. R., & Kumanan, S. (2011). Optimization of parameters of submerged arc weld using non-conventional techniques. Applied soft computing, 11(8), 5198-5204.
4. Elias, E., Deepak, B.B.V.L. Parhi, D R., and Srinivas, J. (2013). Design & Kinematic Analysis of an Articulated Robotic Manipulator, International Journal of Mechanical and Industrial Engineering, 3(1), 105-108.
5. Gao, X. D., & Na, S. J. (2005). Detection of weld position and seam tracking based on Kalman filtering of weld pool images. Journal of manufacturing systems, 24(1), 1-12.
6. Katherasan, D., Elias, J. V., Sathiya, P., & Haq, A. N. (2014). Simulation and parameter optimization of flux cored arc welding using artificial neural network and particle swarm optimization algorithm. Journal of Intelligent Manufacturing, 25(1), 67-76.
7. Kiddee, P., Fang, Z., & Tan, M. (2014, July). Visual recognition of the initial and end points of lap joint for welding robots. In Information and Automation (ICIA), 2014 IEEE International Conference on (pp. 513-518). IEEE.
8. Kim, I. S., Son, J. S., Kim, I. G., Kim, J. Y., & Kim, O. S. (2003). A study on relationship between process variables and bead penetration for robotic CO 2 arc welding. Journal of Materials Processing Technology, 136(1), 139-145.
9. Kumar, K. K., Srinath, A., Anvesh, G. J., Sai R. P. and Suresh, M. (2013). Kinematic analysis and simulation of 6- DOF KUKAKr5 robot for welding application, International journal of Engineering Research and Applications, 3(2), 820-827.
10. Nagesh, D. S., & Datta, G. L. (2010). Genetic algorithm for optimization of welding variables for height to width ratio and application of ANN for prediction of bead geometry for TIG welding process. Applied soft computing, 10(3), 897-907.
11. Parhi, D. R., Deepak, B. B. V. L., Nayak, D., & Amrit, A. (2012). A. Forward and Inverse Kinematic Models for an Articulated Robotic Manipulator, International Journal of Artificial Intelligence and Computational Research, 4(2), 103-109
12. Xue, Y., Kim, I. S., Son, J. S., Park, C. E., Kim, H. H., Sung, B. S., & Kang, B. Y. (2005). Fuzzy regression method for prediction and control the bead width in the robotic arc-welding process. Journal of Materials Processing Technology, 164, 1134-1139.
13. Ye, Z., Fang, G., Chen, S., & Zou, J. J. (2013). Passive vision based seam tracking system for pulse-MAG welding. The International Journal of Advanced Manufacturing Technology, 67(9-12), 1987-1996.
14. Yoo, W. S., & Na, S. J. (2003). Determination of 3-D weld seams in ship blocks using a laser vision sensor and a neural network. Journal of manufacturing systems, 22(4), 340-347.